INTERNATIONAL JOURNAL OF HYDROGEN ENERGY XXX (2016) 1–9

Available online at www.sciencedirect.com

ScienceDirect

journal homepage: www.elsevier.com/locate/he

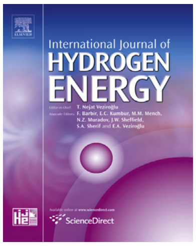

Architectures for scalable integrated photo driven catalytic devices-A concept study[☆]

Simon Kirner [a,*], Peter Bogdanoff [b], Bernd Stannowski [a], Roel van de Krol [b], Bernd Rech [c], Rutger Schlatmann [a]

[a] PVcomB, Helmholtz-Zentrum Berlin, Berlin, Germany
[b] Institute for Solar Fuels, Helmholtz-Zentrum Berlin, Berlin, Germany
[c] Institute for Silicon-Photovoltaics, Helmholtz-Zentrum Berlin, Berlin, Germany

ARTICLE INFO

Article history:
Received 19 February 2016
Received in revised form
6 May 2016
Accepted 7 May 2016
Available online xxx

Keywords:
Solar fuels
Photoelectrolysis
Water splitting
Photoelectrocemical (PEC) devices
Device architectures
Techno-economic analysis

ABSTRACT

Architectures with various degrees of integration are investigated for water splitting devices using the energy of light for fuel production. The many approaches presented in literature for such 'photo driven catalytic (PDC) devices' are reviewed and discussed in perspective of their scalability to large area. Then, back-of-the-envelope type techno-economic considerations for such systems are presented. Compared to the benchmark, consisting of large electrolyzers coupled to the grid, it was found that PDC devices could be competetive in places with high irradiation, given the assumption that no compromises on system stability have to be made compared to stand-alone PV-systems for electricity generation. In agreement with literature, it was found that the cost of the PV part dominate the hydrogen generation costs, based on today's technology. Thus, device architectures that allow low cost PV (by e.g. avoiding use of costly materials or introducing further inherent loss mechanisms) are considered the most promising ones.

Introduction

The tremendous progress in photovoltaic (PV) installations worldwide in the past decade proves that this technology can provide a great share of clean and affordable electricity to the global energy demand [1]. In fact, studies about ultimate potentials of renewable energy sources reveal that solar conversion is the only source able to fulfill future demand for energy by itself, unlike e.g. wind [2]. However, PV has the inherent drawback that its supply is subject to the cycles of nature (day–night, summer–winter). Thus, affordable storage methods are needed to match the temporal differences to the demand for energy and hydrogen produced by electrolysis can be one of them [3]. The combination of PV with electrolysis to store the energy of light directly in the form of hydrogen is therefore an imperative field of study. Due to the comparatively high costs today, electrolysis is competitive only locally in places where electricity costs are exceptionally low. So far, only small scale systems have been demonstrated [4]. Due to

---

[☆] The research leading to these results received support from Europe's Fuel Cell and Hydrogen Joint Undertaking (FCH2-JU) under Grant Agreement No. [621252], project PECDEMO, and from the Helmholtz Association joint initiative 'Energie System 2050 – A contribution to the Research Field Energy.'

* *Corresponding author.*
E-mail address: simon.kirner@helmholtz-berlin.de (S. Kirner).

http://dx.doi.org/10.1016/j.ijhydene.2016.05.088
0360-3199/© 2016 Hydrogen Energy Publications LLC. Published by Elsevier Ltd. All rights reserved.

Please cite this article in press as: Kirner S, et al., Architectures for scalable integrated photo driven catalytic devices-A concept study, International Journal of Hydrogen Energy (2016), http://dx.doi.org/10.1016/j.ijhydene.2016.05.088

the mentioned rapid and continuing decline in electricity cost from PV, sunny regions in the world could soon offer a great potential for clean and inexpensive hydrogen production – competitive with hydropower and wind. This study aims to contribute to the question if the cost of hydrogen production can be reduced by integrating the PV and electrolysis functionalities in a single monolithic device.

Direct solar-to-hydrogen (STH) conversion, coupling one or more photovoltaic cells (herein referred to as the PV-part) via catalysts to an electrolyte (herein referred to as the EC-part) to split water by using the oxygen- and hydrogen-evolving reactions (OER and HER), without need for further electronics, proved to work on lab scale with STH-efficiencies of up to 18%. The key-components and -processes of such ‘photo driven catalytic (PDC) devices’ are given in Table 1a.

Since the first observation of electrolysis on a semiconductor/electrolyte interface by Fujishima and Honda [5], numerous cell designs were presented in literature. In this study, we first review the fundamental processes, which allow converting and storing the energy of the sun's irradiation in hydrogen. Putting the focus on potentially scalable approaches, we highlight the parasitic influence of ohmic losses that occur both in the PV- as well as in the EC-part. The ohmic losses are in a fundamental trade-off with parasitic shading losses or losses of active area, which become relevant at large areas. Against this background, we discuss different approaches with varying levels of integration of PV- and EC-components as presented in literature. We concentrate on planar (as opposed to particle based) architectures, which potentially allow to generate hydrogen at low cost based on today's technology. Thereby, we only consider approaches, which are potentially wireless (monolithic), but do not limit ourselves to either alkaline or acidic electrolytes. Moreover, we consider both buried junction devices as well as devices that have one or more semiconductor/liquid junctions. The former can be classified as (integrated) PV-electrolysis devices, whereas the latter are called PEC or PEC-PV devices. The nomenclature used in this study is given in Table 1b. The term ‘photo driven catalytic (PDC) device’ was suggested by Jacobsson et al., describing any configuration of a PV-cell or -module in combination with an EC regardless of its level of integration [6]. We classify these PDC devices according to the possibility of scalability and identify inherent loss mechanisms related to optical shading, ohmic losses due to transport of charge carriers both in the PV- and in the EC-part and stability requirements. We highlight the advantages of the superstrate design (meaning light impinges through a transparent substrate), used in thin film device technology, such as the possibility of monolithic electrode connection and low optical losses due to limited catalyst transparency or bubble formation.

Table 1

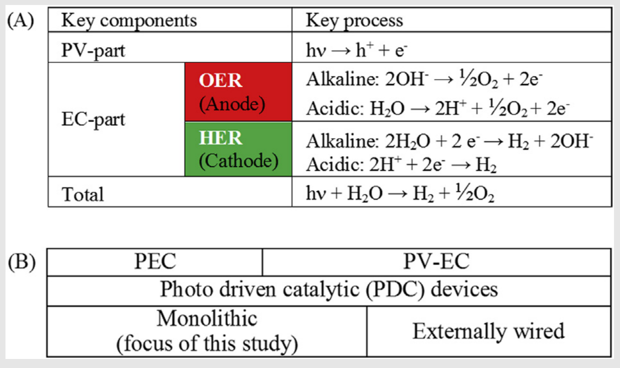

(A)

Key components		Key process
PV-part		$h\nu \rightarrow h^+ + e^-$
EC-part	OER (Anode)	Alkaline: $2OH^- \rightarrow \frac{1}{2}O_2 + 2e^-$ Acidic: $H_2O \rightarrow 2H^+ + \frac{1}{2}O_2 + 2e^-$
	HER (Cathode)	Alkaline: $2H_2O + 2\,e^- \rightarrow H_2 + 2OH^-$ Acidic: $2H^+ + 2e^- \rightarrow H_2$
Total		$h\nu + H_2O \rightarrow H_2 + \frac{1}{2}O_2$

(B)

PEC	PV-EC
Photo driven catalytic (PDC) devices	
Monolithic (focus of this study)	Externally wired

Then, we present back-of-the-envelope techno-economic calculations based on cost estimations for photovoltaic- (PV-) and electrolyzer (EC-) systems presented elsewhere. We conclude that, because the final cost of hydrogen from such systems is likely to be dominated by the cost of electricity (based on today's technology), very limited compromises on the cost of the PV-part can be made, compared to a stand-alone PV system. The largest cost saving potential is thus attributed to an efficient integration of the EC- into the PV-part, without introducing further cost increasing factors (such as the reduction of efficiency through the introduction of further loss mechanisms, the necessity for expensive/rare materials or a reduced system lifetime). For the same reason, we also neglect solar tracking- or concentration-systems, which are today not reducing the cost of PV electricity. Based on the classification and the techno-economic considerations, we propose a device architecture, which should minimize additional cost drivers. Certainly, the results of this study are based only upon a ‘snapshot’ of today's available technology. Future findings in material research might change the results and allow disruptive changes (e.g. emergence of novel, stable wide-bandgap light absorbers or efficient particle based systems).

Fundamentals

Direct hydrogen production by using solar radiation relies on two fundamental processes: First, like in any other electrolyzer, a potential difference larger than the thermodynamic potential of water ($\mu_{th} > 1.23$ eV) has to be applied between cathode and anode. The amount of additional voltage (‘overpotential’) needed depends on the catalysts used as well as the resistive losses occurring in the system. Second, in a *photo driven* catalytic device, light induced splitting of the quasi-Fermi levels in one or more absorbers provides this potential difference. Besides these two processes, other secondary processes such as efficient light in-coupling, transport of charge carriers from absorber to the electrodes, transport of ions between electrodes as well as local separation and collection of reaction products (H_2 and O_2) have to be considered. The current density j_{op} flowing between anode and cathode under operation in such a device, can be used to calculate the solar-to-hydrogen conversion efficiency η_{STH} according to

$$\eta_{STH} = (\mu_{th} \cdot j_{op}) \Big/ P_{irr} \cdot \eta_F \qquad (1)$$

with P_{irr} being the incident irradiance and η_F the Faraday efficiency, which describes the relation between mass of the reaction products and j_{op}. A PDC can be modeled using an

Please cite this article in press as: Kirner S, et al., Architectures for scalable integrated photo driven catalytic devices-A concept study, International Journal of Hydrogen Energy (2016), http://dx.doi.org/10.1016/j.ijhydene.2016.05.088

equivalent circuit such as described by Winkler et al. [7]. Following this approach, we calculate two generator- and load-curves, respectively, given in Fig. 1. Both curves are depicted with two different values for the series resistances to indicate their detrimental influence. For the calculation, we used the 1-Diode equation to describe the current density provided by the PV cell j_{PV}

$$j_{pv}(V) = j_{ph} - j_0\left(\exp\left(\frac{V - R_{s,PV}\cdot j_{PV}}{nV_{th}}\right) - 1\right) - \left(\frac{V - R_{s,PV}\cdot j_{PV}}{R_{p,PV}}\right) \quad (2)$$

.where j_{Ph} is the photo current density, j_0 is the saturation current density, n is the ideality factor, $R_{s,PV}$ the series- and $R_{p,PV}$ the parallel-resistance of the solar cell and V_{th} the thermal voltage[1]. In the lumped $R_{s,PV}$ of a typical solar cell or module, there are depending on the technology (crystalline Silicon (c-Si), CdTe, CIGSe, thin film silicon (TF-Si)) several significant contributions, usually all related to lateral transport. In PV technology, there is a trade-off between j_{Ph} and $R_{s,PV}$. Examples for this are the metal grid coverage in c-Si- [8] or the carrier density in transparent conducting oxides (TCOs) for thin film solar cells [9]. To illustrate this, the generator curve in Fig. 1 with lower $R_{s,PV}$ has a lower j_{Ph}. For inexpensive, large area products, this problem has an economical perspective, as the smallest trade-offs are realized by precious or rare metals such as silver based grids or indium based TCOs. The load curves in Fig. 1 were approximated by the following Tafel expression

$$V = \mu_{th} + \tau_O \log\left(\frac{j_{ec}}{j^O_{ex}}\right) + \tau_H \log\left(\frac{j_{ec}}{j^H_{ex}}\right) + j_{ec}R_{s,EC} \quad (3)$$

where τ_O and τ_H are the Tafel slopes and j^O_{ex} and j^H_{ex} are the exchange current densities of the half reactions (OER and HER), and are labeled accordingly by the respective superscripts “O” and “H”. With these parameters, the overpotential of the catalysts can be described. $R_{s,EC}$ is analog to $R_{s,PV}$ the series resistance parameter, accounting for transport losses in the electrolyte as well as in the ion conducting separator and the catalyst layers.

The operation point is defined by the intersection of the load- and the generator-curve ($j_{op} = j_{EC} = j_{PV}$). Like for $R_{s,PV}$, there are trade-offs to minimize $R_{s,EC}$ -related losses: the PV component can be designed such that it generates higher voltage, e.g. by connecting more than fundamentally needed cells in series, which consequently reduces j_{Ph} [7], the conductivity of the electrolyte can be enhanced by using liquids with more extreme pH values (which usually reduces stability), and/or the lateral dimensions of the unit cell can be tuned to reduce transport distances [10], [11]. An important aspect for realizing small trade-offs is the device architecture. We therefore continue by classifying approaches presented in literature regarding the mentioned problems for scalability.

Solar water splitting systems with varying levels of integration

Several studies dedicated to the classification of PDC devices are present in literature. Modestino and Haussener for example have recently reviewed several device designs and classified them into three major categories, called PEC-, protected photoabsorber- and PV electrolysis-devices [12]. In an earlier study, Jacobsson et al. further divided PDC devices into eight categories, highlighting that the essential mechanisms are the same from one to the other mentioned extremes (PEC to PV-EC) [6]. An excellent overview have also provided Ager et al. [13]. The question which design (if any) will be the most successful *economically* will be judged by the production cost of hydrogen. In this publication, we therefore aim to introduce another classification, which is focused on the scalability of the different design types. We therefore highlight aspects that could induce losses or complicate device-manufacturing, -assembly, -mounting and/or -operation. Among the processes are: shading of the active area, electronic transport between the absorber and the electrodes, separation and transport of product gases from the electrodes to an outlet, transport of the ionic species (in the presence of a gas separator/ion conductor), as well as long term stability. The latter point is frequently addressed in publications, the former often not. We classify five groups depicted in Fig. 2. We classify along two dimensions: Position of electrodes relative to irradiation (‘front-back’, ‘front–front’ or ‘back–back’) and nature of PV-part (‘multi’, multijunction devices, optically *and* electrically monolithically connected in series and ‘series’, single-junction devices only electrically connected in series).

Group (I a) ‘front-back-multi’

The majority of the PEC cells as defined by Modestino and Haussener or Jacobsson et al. fall under this category. They are characterized by the fact that OER and HER occur at the front- and the backside of a planar PV device. In all considered cases, a multijunction solar cell generates the necessary potential. Often, but not necessarily, a wafer (e.g. silicon or gallium arsenide) is used as substrate and at the same time as bottom cell. In all cases, the substrate/PV-part has to allow transversal charge transport from OER to HER. Such devices can theoretically reach STH efficiencies close to 30% [14–16]. Prominent realizations of this design group are e.g. the cell presented by Khaselev and Turner, consisting of a GaInP/GaAs tandem junction exhibiting a STH efficiency of 12% [17], or the GaInP/GaInAs tandem cell recently reported by May et al., elevating the record efficiency to above 14% for this type of device [18]. It is thereby not important in this context if the counter electrode is monolithically attached to the back of the cell, or if it is placed directly behind the cell and connected with a wire to the back contact like in the case of Khaselev and Turner. Therewith, we presume that the backside of the device can be covered (and protected) by the HER catalyst. Another prominent example of this group is the artificial leaf presented by Reece et al., which consists of an amorphous silicon based triple junction solar cell deposited on a conducting (metal) substrate (2.5%) [19] or the device presented by Kelly et al. which achieved more than 7% using the same material [20]. With respect to the product

---

[1] The values in the example are arbitrarily chosen and resemble high quality c-Si solar cells (j_{Ph} = 39 mA/cm^2, $j_0 = 1\cdot10^{-11}$ mA/cm^2, $n = 1$, V_{th} = 25 mV (corresponding to ~25 °C)) and $R_p = 1\cdot10^5$ Ωcm^2. The Tafel slopes and exchange current densities were chosen same as the values published in Ref. [7]: τ_O = 40 mV/dec, τ_H = 30 mV/dec, $j^O_{ex} = 5\cdot10^{-12}$ mA/cm^2 and $j^H_{ex} = 1\cdot10^{-2}$ mA/cm.

Please cite this article in press as: Kirner S, et al., Architectures for scalable integrated photo driven catalytic devices-A concept study, International Journal of Hydrogen Energy (2016), http://dx.doi.org/10.1016/j.ijhydene.2016.05.088

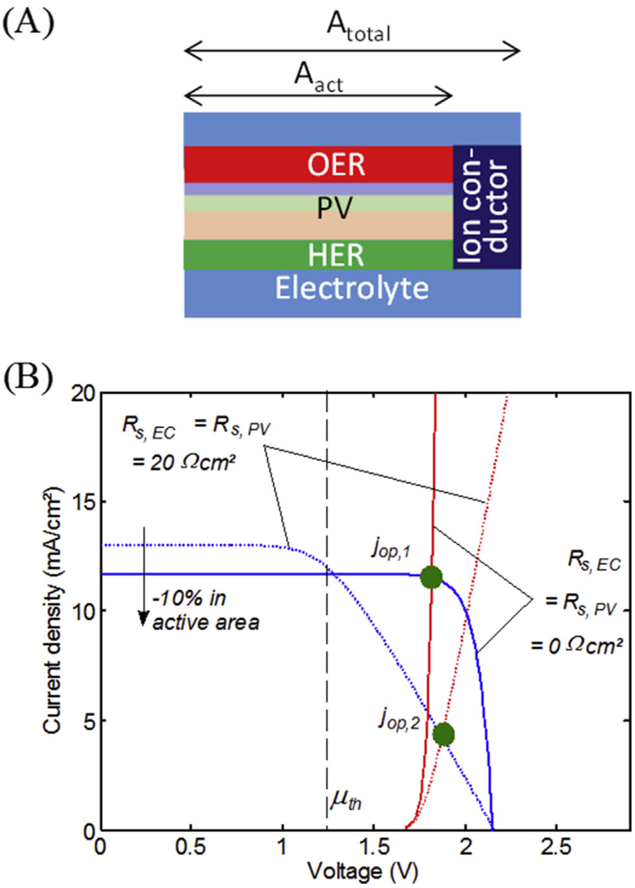

Fig. 1 – (A) Schematic of one of the discussed PDC device architectures with the active and total area of the unit cell indicated. (B) Exemplarily calculated current density voltage characteristics of two PV cells and electrolyzers, respectively, with different active areas and correspondingly different R_s and j_{ph} values.

separation, this design has the inherent advantage that the catalysts are placed on both opposite sides of the substrate, which eases product separation. A disadvantage of this group is that the illumination of the cell is applied through the electrolyte and front electrode. Apart from the fact that neither are perfectly transparent, the appearance of bubbles may induce additional optical losses. For ion transport in large area devices, openings in the PV part have to be realized and filled or covered with a separator to reduce $R_{S,EC}$. According to the introduced inherent trade-off, active area (j_{Ph}) has to be sacrificed for the openings. Haussener et al. and Chen et al. address this optimization issue [10], [11]. Both concluding that a significant area would have to be sacrificed to the openings. An alternative design for this group has recently been suggested by Walczak et al., which reduces the trade-off by tilting the PV part [21]. However, this design is not planar therefore requires solar-tracking and is thus not considered here.

Group (I b) 'front-front-multi'

The next group of cells differs to the first that the counter electrode is placed on the front side of the cell and connected to the back contact via a solid conductor. This design has the advantage that the ionic transport is easier because the distances can be shorter. Therewith, the necessity to sacrifice area to holes allowing ionic transport is reduced. A prominent realization from this group is e.g. the $BiVO_4$/TF-Si multi-junction device presented by Abdi et al. [22]. With a similar device design, recently STH efficiencies of up to 5.2% have been shown [23] [24], which is the highest yet reported efficiency of PEC cells with metal oxide absorbers that are known to be highly stable. Such a design is often used on laboratory scale for measurements performed with an aperture, where the counter electrode can then be placed outside the active area. Consequently, the Reece cell efficiency increased to 4.7%. Regarding fabrication of large area devices, this device has several obvious drawbacks related to the counter electrode: (1) increased manufacturing complexity due to wiring (no monolithic design has been realized to our knowledge). (2) Additional shading and (3) product separation is difficult to realize.

Group (I c) 'front-front-series'

Similar to the previous group, both catalyst sites are located on the front of the device. The difference is that the PV-part does not consist of one monolithic stack, but of (at least two) electrically but not optically in series connected parts. A realization of this architecture was e.g. presented by Smotkin et al. using CdSe and CoS photoelectrode with Pt catalysts [25]. Due to the series connection, the effective current *density* j_{op} relevant for η_{STH} has to be calculated relative to the area of the unit- (i.e. smallest repeatable unit) and not the single-cell. Like in the previous groups, a loss mechanism lies in the illumination through electrolyte and catalyst as well as product separation. In addition, the requirements regarding stability of the materials are high. On the other hand, the advantages for transport of the products of the previous group remain [10].

Group (II a) 'back-back-multi'

Group *(II a)* is characterized by the fact that both contacts are placed on the rear side of the PV device. This can e.g. be realized by deposition of thin films on a transparent substrate and subsequent laser structuring, as it is industrially done for CdTe or TF-Si based solar cells and modules. Another method is using a non-transparent conducting substrate and laying the front contact to the rear side via holes or along the edge to the backside (like in a metal- or emitter-wrap-through multijunction cell). In this configuration, the semiconductor can be separated from the electrolyte easily (e.g. protection layers do not have to transmit light like in previous groups), which presumably allows improved stability. Another advantage is that illumination does not occur through the electrolyte and catalyst layer and no reaction products (bubbles) are in front of the absorber. Probably due to these advantages, the highest yet reported STH efficiency of 18% (at AM0) has been realized in this configuration by Licht et al. using an AlGa/Si tandem solar cell [26]. Using light concentration Fujii et al. showed >12% on a large area including a membrane for product separation [27]. Recently, Urbain et al. have achieved efficiencies of 9.5% using such a configuration with an a-Si:H/a-Si:H/μc-Si:H triple junction solar cell, modified with noble metal

Please cite this article in press as: Kirner S, et al., Architectures for scalable integrated photo driven catalytic devices-A concept study, International Journal of Hydrogen Energy (2016), http://dx.doi.org/10.1016/j.ijhydene.2016.05.088

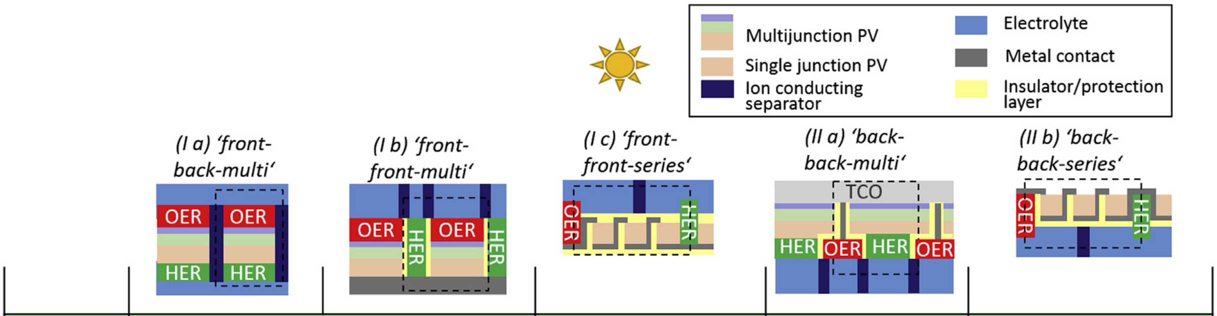

	(I a) 'front-back-multi'	(I b) 'front-front-multi'	(I c) 'front-front-series'	(II a) 'back-back-multi'	(II b) 'back-back-series'
Advantages	Efficiency potential			Efficiency potential	
	Product separation	Ion transport			
				Stability, Compatibility with existing PV technology	
Challenges	Stability of semiconductors/electronic properties of stable oxides Optical shading from electrolyte, catalysts, bubbles		Lateral transport in TCO or metal grid on front side		
	Ion transport	Product separation, Cell-to-electrode interconnect (active area loss)			
			Cell-to-cell interconnect (active area), high local current density		Cell-to-cell interconnect (active area loss) high local current density
Reported Realizations	14% **III/V 2J** *May et al [18]*, 12.3% **III/V 2J** *Khaselev et al [17]*	5.2% **$BiVO_4$/TF-Si 3J** *Han et al [23]*, 4.7% **TF-Si 3J** *Reece et al [19]*	1% **CdSe+CoS** *Smotkin et al [25],*	18.3% **III/V 2J** *Licht et al [26]*, 9.5% **TF-Si 3J** *Urbain et al [28]*	10% **4xSi** *Cox et al [29]*, 10% **3xCIGSe** *Jacobsson et al [33]*, 12.3% **2xPVK** *Luo et al [34]*

Fig. 2 – Overview of the discussed PDC device architectures. OER and HER can be additional layers (like Pt or RuO_2), or the semi-conductor electrolyte interface, photoactive- or passive (dark-) catalysts, transparent or opaque. Position of OER and HER can be exchanged in some cases to account for n/p versus p/n PV devices. Unit cells are marked by dashed box. Illumination occurs always from top.

catalysts [28]. Stellmach et al. have reached 2.5% with the noble metal free HER catalyst MoS_2 catalyst in a complete wireless 'artificial leaf' configuration [29]. According to the classification of Modestino and Haussener, such a device would be labeled a PV/electrolysis device [12], although it could be in principle fabricated entirely monolithic. In the classification performed by Jacobsson et al., such a device does not appear and could be placed anywhere between configuration (a) and (f) because it can be placed outside the electrolyte for one but could be entirely monolithic on the other hand [6]. Lateral electronic transport on the front side is an inherent loss mechanism that has to be considered. Presented conductors are TCOs, like in a CdTe or TF-Si superstrate modules, or highly doped emitter layers like shown by Licht et al. A drawback of this design is that both products are being generated at the same side. This reduces the available active catalytic area for planar systems and complicates the product separation. Both drawbacks induce the necessity to structure the backside of the PV part. A possible solution are micro fluid type reactors where both catalysts are being placed right next to each other separated by ion conducting membranes/diaphragms [30]. In this design, the losses occurring due to TCO sheet-, electrolyte- and membrane-resistivity have to be balanced with optical losses induced by the loss of active area due to the interconnection. In fact, for charge carrier transport in this architecture, presumably very similar design criteria as calculated by Haussener et al. for *Group (I a)* apply.

Group (II c) 'back-back-series'

Group (II c) comprises of series connected single junction solar cells designed to achieve optimal operating voltages. The concept still allows wireless combinations and no DC/DC converter is necessary, which could provide a significant cost advantage (see further discussion below). Miller et al. call this type of device "area matched integrated PV-electrolyzer system" meaning that area and interconnection scheme are optimized such that the operating voltage is above V_{th} [31]. Winkler et al. have described the optimization process using the above introduced model. They show that depending on the output voltage of the solar cell, the electrolyte conductance, as well as the over potentials of the catalysts, the ideal number of single junction solar cells varies strongly: Assuming ideal PV- and EC-parts (i.e. $V_{mpp} = \mu_{th}$), a single cell with $E_g = 1.34$ eV could operate at >30% STH efficiency [7]. Considering more realistic situations, maximum efficiency for a single junction cell drops <12%, due to the high required band gap [16] and thus more cells are needed for less ideal EC conditions. Regarding experimental realizations: Cox et al. have recently shown a STH efficiency of 10% using a module comprised of four commercially available Si solar cells with adjusted area connected in series to non-precious catalysts [32]. A similar high STH efficiency of ~10% report Jacobsson et al. from a CIGSe module composed of three cells monolithically connected in series with two Pt electrodes [33]. More

Please cite this article in press as: Kirner S, et al., Architectures for scalable integrated photo driven catalytic devices-A concept study, International Journal of Hydrogen Energy (2016), http://dx.doi.org/10.1016/j.ijhydene.2016.05.088

recently, 12.3% have been reported by series connection of *two* Perovskite solar cells with non-noble catalysts [34].

The reported Si- as well as the CIGSe 'series connected' approaches have the drawback that they use a substrate configuration. This means light enters through the PV not the substrate, as opposed to superstrate configuration where the PV part is illuminated through a transparent substrate. Therefore, when considering large area devices, the substrate has to be macroscopically interrupted to connect the PV electrodes to the catalysts or long distances have to be bridged by wiring. In the superstrate configuration, such an interruption is less area consuming because it can be made monolithically by means of a laser, like in thin film silicon modules. Besides thin film silicon, CdTe and some organic solar cells (also PVK) are typically made in this configuration and recently also CIGSe solar cells in superstrate configuration have shown efficiencies above 11% [35]. In such a superstrate design, the in *(II a)* mentioned advantages of easy electrolyte/semiconductor separation (stability) and low optical losses due to direct illumination apply. However, a drawback compared to *(II a)*, based devices is the necessity for cell-to-cell interconnection, which induces further active area losses. Another technological drawback of any series connected compared to true multijunction approach is the higher local current density, which make them more prone to ohmic losses.

Economic considerations

The benchmark for hydrogen production from integrated PDC devices is the cost per kg-H_2 of PV-EC systems with converters. A cost comparison between these systems, has to be based on the levelized cost, which account for the entire costs that accumulate over the lifetime including investment and capital cost, cost for maintenance and operation, component lifetimes etc.. In the following, we compare four cases: (scenario A) is the case of a large EC unit coupled to a large PV system. Such systems reach reported efficiencies above 12% [36] and much higher efficiencies are principally possible. They have the advantage that they can be coupled to batteries or connected to the grid, which allows a steady operation of the EC and unwanted gas crossover, due to shut down of the electrolysis, can be avoided. Furthermore, maximum power point tracking could be used. On the other hand, integrated systems have the advantage of thermal coupling of PV and EC, which can result in a positive temperature coefficient [37]. Idle cycling is a problem for EC units, as it can lead to oxygen reduction at the cathode and/or water formation from product recombination at the anode. (Scenario B) is the case of a system based on integrated PDC devices, from cost estimations based on EC-units. Scenario C is the optimistic case, where we assume a decrease of 50% for the EC costs due to the integration. In scenario D, additionally the system lifetime is reduced by 50%. We highlight that the aim of this study is not an accurate prediction of the system performance, but to give a rough benchmark that integrated systems would have to reach in order to be competitive to the decoupled approach (with inverter).

Good cost estimations for scenario A can be made, as the components are readily available on large scale and several studies exist providing cost estimations for the near future. For the cost of PV electricity, e.g. the levelized cost of electricity (LCOE) are estimated by the international technology roadmap for photovoltaics (ITRPV) edition published in 2015. The cost estimations in the ITRPV are based on the expertise of 30 contributors from the PV community including academia, PV-cell, -module and equipment-manufacturers. LCOE for a large system located in a sunny region (2000 kW h/m^2/year) are \$0.049/kWh, assuming the cost structure of 2015 [38]. The study gives a break down, indicating that the module make up 58–63% of the cost. For large electrolysis reactors, also several cost studies exist. A recent overview give Mergel et al. [39]. According to a study from NREL published in 2009, the cost for hydrogen generated by a centralized 100 MW electrolyzer powered via the grid from renewable sources (wind) was in 2009 in the United States \$2.70/kg-H_2. The largest cost fraction (>76%) consists of the electricity costs, which were assumed to be \$0.045/kWh [40]. The capital cost, making up the second largest fraction (16%) were assumed to be \$380/kW. A similar cost range was found by a more recent German study: The authors of the NOW study estimated the hydrogen production price to be at €3.85/kg-H_2 for a 870 kW PEM electrolyzer operated only 35% of the time, with electricity purely generated by wind at a cost of €0.03/kWh [41]. Due to the low assumed EC utilization in this study, the fraction of fix costs is much larger with 55% for assumed investment costs of €800/kW. Costs for operation besides electricity and maintenance are in all scenarios <5%.

Regarding the cost of integrated PV- EC-systems, there are estimations given by Rodriguez et al. [42]. For a system located in Arizona (USA, ~2000 kWh/m^2/year), they calculate the levelized cost of hydrogen production (LCHP) to be as low as \$2.90/kg-H_2 for concentrated PV (CPV). In this study however, the authors assume very low PV electricity generation costs of \$0.02/kWh, which is less than half of the value given in the above-mentioned ITRPV study. Interestingly, the electricity costs still make up 97% of the LCHP. At this high fraction of the PV part to the LCHP, it is questionable whether CPV would be employed, because of its typically higher LCOE [43]. Moreover, *in this study* we argue that the degrees of freedom to increase the cost of the LCOE from the PV part are very limited. However, the authors show very nicely that the *economically* optimized area fraction of catalyst to PV is <10% for catalysts such as Ni or Co_2O_3. This is interesting in the context of our paper because it further reduces the necessity to illuminate the PV through the catalysts and the electrolyte.

Such bottom-up calculations for the LCHP based on the cost of the single components of the system as performed by Rodriguez et al., we compare to back-of-the-envelope type calculations based on the above described data for complete, readily available PV- and EC-systems in Fig. 3. The LCHP are depicted as a function of 'effective usage (hours/year)'. These depend on the local irradiation as well as the yield of the PV part. A first order approximation is kWh/m^2 = kWh/kWp. The input data is given in Table 1 and will be now discussed in detail. Scenario A is the case of a PV-system coupled to an EC via a DC/DC converter. Therein, we used the PV costs given in Ref. [38] (€1150/kW) and the EC investment and maintenance

Please cite this article in press as: Kirner S, et al., Architectures for scalable integrated photo driven catalytic devices-A concept study, International Journal of Hydrogen Energy (2016), http://dx.doi.org/10.1016/j.ijhydene.2016.05.088

costs for a large PEM unit as predicted by Smolinka et al. [41] under the assumption that the electricity is provided completely by the PV unit. The NOW study, assumes a comparatively long EC component lifetime of 25 years, compared to Rodriguez et al., which estimate a lifetime of only 10 years. The data for the capital cost are based on [38] and are assumed to be equal for PV and EC for simplicity.

For the case without a converter (scenario B), we start from the cost break-down for large PV-systems in Asia given in Ref. [38], we estimate the cost of the PV to be €1045/kW. Therein, we accounted for the absence of an inverter (−11%) and wiring (−7%). Optimistically, we estimated the STH efficiency to be only 50% lower than for PV alone. Thus, increased the demand for land and mounting by this factor, which results in an increase of 9%. In this scenario, the EC unit costs remain the same as in scenario A, resulting in only a marginal cost reduction. It has to be kept in mind however, that, as mentioned above, scenario A still has the advantage that a shut-down of the EC (e.g. at night times) can be avoided by applying external power. A completely (wire-less) integrated device does not have this possibility. It can be seen in Table 2 that the EC makes up 46% of the investment costs.

Scenario C is the positive scenario for integrated approaches and motivated by the following considerations: First, we assume that the PV part of an integrated device could provide in the best-case electricity at the same costs as a large PV system (i.e. PV part of the investment costs remains same as in B). Therefore, no further cost reductions are assumed in this part. This assumption might be arguable, as e.g. the electrolyte could cool the PV and therewith enhance yield, however, given the above-described limitations (e.g. reduced stability, reduction of active area due to interconnects, etc.); we believe this is still a reasonably positive assumption. Furthermore, we argue that considerable cost reductions are possible merely by integrating EC and PV into one device. Another argument for this is the difference in market penetration of the two technologies: PV provided 139 TW h/year in 2013 compared to an equivalent energy/year of about 0.09 TW h/year (2007) converted into H_2 by EC [1], [44]. Therefore, we allowed the EC costs in scenario C to be lower by −50%. With this measure, the costs come down into the range predicted by Rodriguez et al. as shown in Fig. 3. As mentioned above, in scenario D we reduced the system lifetime by 50%. Today, highly integrated designs show a low lifetime because the electrolyte affects the semi-conductor and efficient sealing concepts have not been developed yet. In particular, systems with a direct semi-conductor liquid junction have stability problems. Devices where HER and OER are placed on the rear side have the advantage that opaque sealing layers can be used. In the model, the reduced system lifetime overcompensates the investment cost reductions by far and the Scenario D has the highest LCHP.

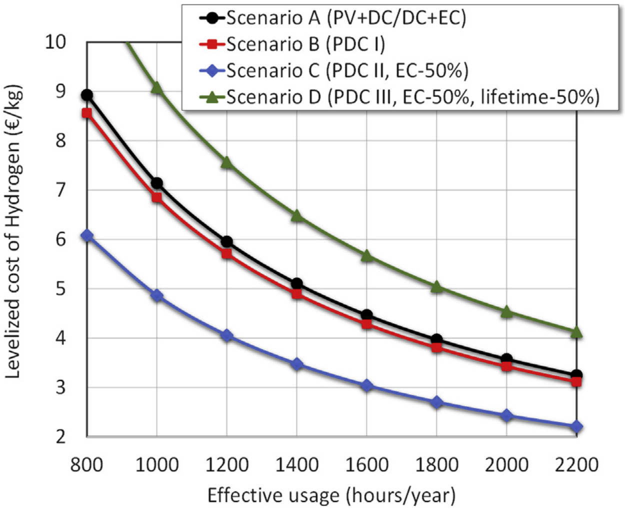

Fig. 3 – Cost estimations based in the three described scenarios as a function of effective usage, depending on the local irradiation.

Table 2 – Input parameters (changes between the different scenarios are marked *italic*).

PV	
Systemsize (kWp)	1000
Price incl. ground/mounting (€/kWp) as given by ITRPV [37] (scenario A)	1150
Price incl. increased land usage, no AC/DC, no wiring (scenarios B – D)	1045
Years of operation (a) (scenarios A – C)	25
Years of operation (a) (scenario D)	12.5
Linear degradation (%kWp/a)	1%
EC	
Systemsize = PV (kWp)	1000
Price incl. delivery/installation (€/kWp)	880
as given by NOW [40] (scenarios A – B)	
Price assuming EC-cost -50% (e.g. due less expensive parts) (scenarios C – D)	440
Years of operation (a) (scenarios A – C)	25
Years of operation (a) (scenario D)	12.5
Linear degradation (%kWp/a)	1%
Maintenance, operations and insurance (%invest/a)	4%
Faraday efficiency	82%
Capital Costs	
Share debt	80%
Interest rate	5%
Loan tenor (a)	20

Now we discuss how cost reductions could be materialized. The largest cost fractions in electrolyzers consist of the rectifier, the membrane electrode assembly (including ion separator), bipolar plates and current collectors [44]. In future integrated photo driven catalytic devices, many of the parts could become obsolete. Structuring methods applied for the PV-part, such as laser structuring or screen printed contacts, could be used for the EC and this way the number of total process steps as well as substrate, mounting cost etc. could be reduced. Fig. 4 shows a possible scalable device architecture, which is based on the above discussed superstrate configuration and similar to micro fluid devices suggested by Modestino et al. [30]. Recently, Turan et al. have presented a module scaled to 64 cm^2 in a similar design based on series connected thin film solar cells [45]. Using three or four junction thin film silicon cells, which allow high operating voltages above 2 V [46], we expect STH efficiencies in the range of 10% to be feasible on large area. Semiconductor and electrolyte could be separated by means of thin (transversally conducting) protection layers such as TiO_2 [47]. Since the

Please cite this article in press as: Kirner S, et al., Architectures for scalable integrated photo driven catalytic devices-A concept study, International Journal of Hydrogen Energy (2016), http://dx.doi.org/10.1016/j.ijhydene.2016.05.088

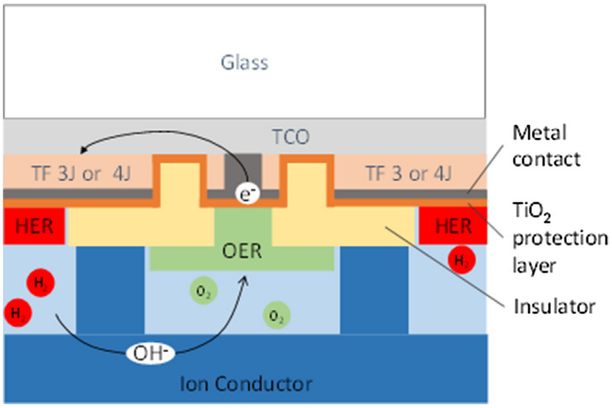

Fig. 4 – A new PDC superstrate based device architecture based on TF–Si PV with 3 or 4 junctions.

electrolyte is placed on the back, the transparency requirement of the protection layer is obsolete. Insulator, as well as HER- and OER-catalysts could be conveniently deposited and structured using known technologies as screen-printing. The device design is also applicable for various other solar cell- and module-designs that allow putting electron and hole contacts on the rear side, such as CdTe-modules or wafer-based emitter wrap through approaches.

Conclusions

We have discussed the trade-off between active area losses and low series-resistances, which become relevant for large area photovoltaic as well as photo driven catalytic (PDC) devices. In this context, we have classified various approaches for PDC devices and have pointed out the multiple advantages of superstrate multijunction configurations. These are direct illumination (no optical losses due to electrolyte, catalyst or bubbles), easy separation of semiconductor and electrolyte (stability) as well as short transport distances for ions and the absence of cell-to-cell interconnection losses. By means of basic techno-economic considerations and back-of the envelope calculations, we conclude that the LCHP will be dominated by the LCOE of the PV-part based on today's technology. Therefore, we conclude that little compromises in terms of cost per kWp can be made on the PV-side of a PDC. However, further cost reductions compared to completely decoupled systems with converters seem feasible on the EC-side. Finally, we propose a new superstrate PV based device architecture that is in principle applicable for various PV technologies, which should be easily fabricatable at low costs.

REFERENCES

[1] IEA. Technology roadmap solar photovoltaic energy. IEA/OECD, Tech. Rep.. 2014. available online https://www.iea.org/publications/freepublications/publication/pv_roadmap.pdf.

[2] Deng YY, Haigh M, Pouwels W, Ramaekers L, Brandsma R, Schimschar S, et al. Quantifying a realistic, worldwide wind and solar electricity supply. Glob Environ Change 2015;239:252.

[3] IEA. Technology roadmap hydrogen and fuel cells. IEA/OECD, Tech. Rep.. 2014. available online http://www.iea.org/publications/freepublications/publication/TechnologyRoadmapHydrogenandFuelCells.pdf.

[4] Rekioua D, Bensmail S, Bettar N. Development of hybrid photovoltaic-fuel cell system for stand-alone application. Int J Hydrogen Energy 2014;39:1604.

[5] Fujishima A, Honda K. Photolysis-decomposition of water at the surface of an irradiated semiconductor. Nature 1972;238:37.

[6] Jacobsson TJ, Fjallstrom V, Edoff M, Edvinsson T. Sustainable solar hydrogen production: from photoelectrochemical cells to PV-electrolyzers and back again. Energy Environ Sci 2014;7:2056.

[7] Winkler MT, Cox CR, Nocera DG, Buonassisi T. Modeling integrated photovoltaic–electrochemical devices using steady-state equivalent circuits. Proc Nat Acad Sci 2013;110:E1076.

[8] Green MA. Solar cells: operating principles, technology, and system applications. Englewood Cliffs NJ: Prentice-Hall Inc.; 1982.

[9] Ellmer K. Past achievements and future challenges in the development of optically transparent electrodes. Nat Photonics 2012;6:809.

[10] Haussener S, Xiang C, Spurgeon JM, Ardo S, Lewis NS, Weber AZ. Modeling, simulation, and design criteria for photoelectrochemical water-splitting systems. Energy Environ Sci 2012;5:9922.

[11] Chen Y, Xiang C, Hu S, Lewis NS. Modeling the performance of an integrated photoelectrolysis system with 10 × solar concentrators. J Electrochem Soc 2014;161:F1101.

[12] Modestino MA, Haussener S. An integrated device view on photo-electrochemical solar-hydrogen generation. Ann Rev Chem Biomol Engin 2015;6:13.

[13] Ager JW, Shaner MR, Walczak KA, Sharp ID, Ardo S. Experimental demonstrations of spontaneous, solar-driven photoelectrochemical water splitting. Energy Environ Sci 2015;8:2811.

[14] Hu S, Xiang C, Haussener S, Berger AD, Lewis NS. An analysis of the optimal band gaps of light absorbers in integrated tandem photoelectrochemical water-splitting systems. Energy Environ Sci 2013;6:2984.

[15] Haussener S, Hu S, Xiang C, Weber AZ, Lewis NS. Simulations of the irradiation and temperature dependence of the efficiency of tandem photoelectrochemical water-splitting systems. Energy Environ Sci 2013;6:3605.

[16] Pinaud BA, Benck JD, Seitz LC, Forman AJ, Chen Z, Deutsch TG, et al. Technical and economic feasibility of centralized facilities for solar hydrogen production via photocatalysis and photoelectrochemistry. Energy Environ Sci 2013;6:1983.

[17] Khaselev O, Turner JA. A monolithic photovoltaic-photoelectrochemical device for hydrogen production via water splitting. Science 1998;280:425.

[18] May MM, Lewerenz H-J, Lackner D, Dimroth F, Hannappel T. Efficient direct solar-to-hydrogen conversion by in situ interface transformation of a tandem structure. Nat Comm 2015;6:8286.

[19] Reece SY, Hamel JA, Sung K, Jarvi TD, Esswein AJ, Pijpers JJH, et al. Wireless solar water splitting using silicon-based semiconductors and earth-abundant catalysts. Science 2011;334:645.

[20] Kelly NA, Gibson TL. Design and characterization of a robust photoelectrochemical device to generate hydrogen using solar water splitting. Int J Hydrogen Energy 2006;31:1658.

Please cite this article in press as: Kirner S, et al., Architectures for scalable integrated photo driven catalytic devices-A concept study, International Journal of Hydrogen Energy (2016), http://dx.doi.org/10.1016/j.ijhydene.2016.05.088

[21] Walczak K, Chen Y, Karp C, Beeman JW, Shaner M, Spurgeon J, et al. Modeling, simulation, and fabrication of a fully integrated, acid-stable, scalable solar-driven water-splitting system. ChemSusChem 2015;8:544.

[22] Abdi FF, Han L, Smets AH, Zeman M, Dam B, van de Krol R. Efficient solar water splitting by enhanced charge separation in a bismuth vanadate-silicon tandem photoelectrode. Nat Comm 2013;4:2195.

[23] Han L, Abdi FF, van de Krol R, Liu R, Huang Z, Lewerenz H-J, et al. Efficient water-splitting device based on a bismuth vanadate photoanode and thin-film silicon solar cells. ChemSusChem 2014;7:2832.

[24] Azarpira A, Pfrommer J, Olech K, Hohn C, Driess M, Stannowski B, et al. Optimized immobilization of ZnO: Co electrocatalysts realizes 5% efficiency in photo-assisted splitting of water. J Mater Chem A 2016;4:3082.

[25] Smotkin ES, Cervera-March S, Bard AJ, Campion A, Fox MA, Mallouk T, et al. Bipolar Cadmium Selenide/Cobalt(ii) Sulfide semiconductor photoelectrode arrays for unassisted photolytic water splitting. J Phys Chem 1987;91:6.

[26] Licht S, Wang B, Mukerji S, Soga T, Umeno M, Tributsch H. Over 18 solar energy conversion to generation of hydrogen fuel; theory and experiment for efficient solar water splitting. Int J Hydrogen Energy 2001;26:653.

[27] Fujii K, Nakamura S, Sugiyama M, Watanabe K, Bagheri B, Nakano Y. Characteristics of hydrogen generation from water splitting by polymer electrolyte electrochemical cell directly connected with concentrated photovoltaic cell. Int J Hydrogen Energy 2013;38:14424.

[28] Urbain F, Smirnov V, Becker J-P, Lambertz A, Yang F, Ziegler J, et al. Multijunction Si photocathodes with tunable photovoltages from 2.0 V to 2.8 V for light induced water splitting. Energy Environ Sci 2016;9:145.

[29] Bogdanoff P, Stellmach D, Gabriel O, Stannowski B, Schlatmann R, van de Krol R, et al. Artificial leaf for solar water splitting based on a triple–junction a-Si-μc-Si thin film solar cell and a pedot:pss/catalyst blend. Energy Tech 2016;4:230.

[30] Modestino MA, Diaz-Botia CA, Haussener S, Gomez-Sjoberg R, Ager JW, Segalman RA. Integrated microfluidic test-bed for energy conversion devices. Phys Chem Chem Phys 2013;15:7050.

[31] Miller EL, DeAngeils A, Mallory S. Multijunction approaches to photoelectrochemical water splitting. In: van de Krol R, Grätzel M, editors. Photoelectrochemical hydrogen production. Heidelberg: Springer; 2012. p. 205–76.

[32] Cox CR, Lee JZ, Nocera DG, Buonassisi T. Ten-percent solar-to-fuel conversion with nonprecious materials. Proc Nat Acad Sci 2014;111:14057.

[33] Jacobsson TJ, Fjallstrom V, Sahlberg M, Edoff M, Edvinsson T. A monolithic device for solar water splitting based on series interconnected thin film absorbers reaching over 10% solar-to-hydrogen efficiency;. Energy Environ Sci 2013;6:3676.

[34] Luo J, Im J-H, Mayer MT, Schreier M, Nazeeruddin MK, Park N-G, et al. Water photolysis at 12.3 efficiency via perovskite photovoltaics and earth-abundant catalysts. Science 2014;345:1593.

[35] Heinemann MD, Efimova V, Klenk R, Hoepfner B, Wollgarten M, Unold T, et al. Cu(In,Ga)Se2 superstrate solar cells: prospects and limitations. Prog Photov Res Appl 2014;23:1228.

[36] Gibson TL, Kelly NA. Optimization of solar powered hydrogen production using photovoltaic electrolysis devices. Int J Hydrogen Energy 2008;33:5931.

[37] Urbain F, Becker JP, Smirnov V, Ziegler J, Yang F, Kaiser B, et al. Influence of the operating temperature on the performance of silicon based photoelectrochemical devices for water splitting. Mater Sci Semicond Proc 2016;42:142.

[38] 2014 results International technology roadmap for photovoltaic (IRTPV). 6th ed. 2015. Available online http://www.itrpv.net/Reports/Downloads/2015/.

[39] Mergel J, Carmo M, Fritz D. Status on technologies for hydrogen production by water electrolysis. Wiley-VCH Verlag GmbH & Co. KGaA; 2013. p. 423–50. Available online, http://dx.doi.org/10.1002/9783527673872.ch22.

[40] Genovese J, Harg K, Paster M, Turner J. Current state-of-the-art hydrogen production cost estimate using water electrolysis. NREL; 2009. Tech. Rep., 2009, Available online, http://www.hydrogen.energy.gov/pdfs/46676.pdf.

[41] Smolinka T, Günther M, Garche J. Stand und Entwicklungspotenzial der Wasserelektrolyse zur Herstellung von Wasserstoff aus regenerativen Energien. NOW, Tech. Rep.. 2011. Available online http://de.scribd.com/doc/74681539/Technologie-Der-Wasserelektrolyse-Abschlussbericht-Frauenhofer-ISE#scribd.

[42] Rodriguez CA, Modestino MA, Psaltis D, Moser C. Design and cost considerations for practical solar-hydrogen generators. Energy Environ Sci 2014;7:3828.

[43] Haysom JE, Jafarieh O, Anis H, Hinzer K, Wright D. Learning curve analysis of concentrated photovoltaic systems. Prog Photov Res Appl 2015;23:1678.

[44] Bertuccioli L, Chan A, Hart D, Lehner F, Madden B, Standen E. Study on development of water electrolysis in the EU. Tech. Rep. E4tech and Element Energy; 2014. Available online http://www.fch.europa.eu/sites/default/files/study%20electrolyser_0-Logos_0_0.pdf.

[45] Turan B, Becker JP, Urbain F, Finger F, Rau U, Haas S. From leaf to tree: upscaling of artificial photosynthesis. Mater Sci 2016. Available online, http://arxiv.org/abs/1604.03074.

[46] Kirner S, Neubert S, Schultz C, Gabriel O, Stannowski B, Rech B, et al. Quadruple-junction solar cells and modules based on amorphous and microcrystalline silicon with high stable efficiencies. Jap J Appl Phys 2015;54:08KB03.

[47] Hu S, Shaner MR, Beardslee JA, Lichterman M, Brunschwig BS, Lewis NS. Amorphous TiO2 coatings stabilize Si, GaAs, and gap photoanodes for efficient water oxidation. Science 2014;344:1005.

Please cite this article in press as: Kirner S, et al., Architectures for scalable integrated photo driven catalytic devices-A concept study, International Journal of Hydrogen Energy (2016), http://dx.doi.org/10.1016/j.ijhydene.2016.05.088